
Article:
Zhu, C. orcid.org/0000-0002-5516-661X, Hobbs, M. orcid.org/0000-0003-4661-692X and Willmott, J.R. orcid.org/0000-0002-4242-1204 (2020) An accurate instrument for emissivity measurements by direct and indirect methods. Measurement Science and Technology, 31 (4). ISSN 0957-0233

https://doi.org/10.1088/1361-6501/ab5e9b

An accurate instrument for emissivity measurements by direct and indirect methods

To cite this article before publication: Chengxi Zhu *et al* 2019 *Meas. Sci. Technol.* in press https://doi.org/10.1088/1361-6501/ab5e9b

IOP Publishing Measurement Science and Technology
Meas. Sci. Technol. **XX** (XXXX) XXXXXX https://doi.org/XXXX/XXXX

An Accurate Instrument for Emissivity Measurements by Direct and Indirect Methods

Chengxi Zhu, Matthew J. Hobbs and Jon R. Willmott

Department of Electronic and Electrical Engineering, University of Sheffield, Sheffield, United Kingdom

E-mail: j.r.willmott@sheffield.ac.uk

Received xxxxxx
Accepted for publication xxxxxx
Published xxxxxx

Abstract

Emissivity is a quantity essential to consider when assessing the measurement uncertainty in non-contact temperature measurements. This paper presents a new instrument for measuring emissivity of opaque materials from 200 to 450 °C in the spectral range of 2.1 to 2.5 μm. These ranges are ideal for measuring the temperature of metals, such as aluminium, during manufacture or heat-treating process. The instrument consists of a pair of hemispherical cups coated with Vantablack® and gold respectively, a custom designed radiation thermometer, and a hot plate. This instrument enables both the direct and the indirect methods for measuring emissivity of materials. Use of two identical cups allowed for quantitative analysis of the uncertainty of the instrument to determine the most suitable emissivity measurement range. The expanded uncertainty of the instrument was lower than 0.058 (k = 2) over the entire measuring temperature range. Studies were undertaken using different materials with emissivities ranging from 0.06 to 1. These included: aluminium alloy 6082, stainless steel 304, and HiE-Coat 840M paint. Relative uncertainty analysis indicated that the indirect method was more accurate for measuring low emissivity materials, whereas the direct method was more suitable for all other materials. Our instrument, with experimentally determined measurement uncertainty, aims to offer accurate emissivity references for use in radiation thermometry applications.

Keywords: emissivity, infrared, radiation thermometry, uncertainty

1. Introduction

Emissivity can be considered as the efficiency factor of thermal radiation emitted from the surface of an object. Planck's Law describes the emission of a theoretical object, known as a blackbody, whose emissivity is 1 and all real objects radiate with emissivity lower than this figure. Non-contact temperature measurement instruments are calibrated against approximate blackbody radiators. Thus, it is essential to hold a priori information of a measurand's emissivity when making a non-contact temperature measurement with a radiation thermometer or thermal imaging camera. Emissivity is used as a factor to adjust the radiance temperature measured by an instrument to absolute temperature [1-3]. The measurement uncertainty of radiation thermometry is determined by both the accuracy of the instruments themselves and the uncertainty of a priori emissivity information [4]. Therefore, failing to acquire accurate emissivity information can be deleterious to measurement uncertainty [5]. Emissivity is a spectral directional quantity obtained by comparing the radiance from the body of interest to that from a blackbody at the same temperature and viewing conditions. Emissivity is also affected by the surface condition of an object, including the chemical composition and surface

topography [6]. At present, emissivity is primarily measured by experimental methods that require accurate and traceable measurement instruments [7-9].

Various forms of instruments have been developed and demonstrated for the measurement of emissivity. These can be classified into the direct and indirect measurement methods. The direct method measures emissivity by calculating the ratio of the radiant power from an object of interest to that from a blackbody under the same measurement conditions [10, 11]. The indirect method first measures the reflectivity and transmissivity of an object of interest, assuming it is not opaque. The emissivity can then be calculated based on Kirchhoff's law [12-14]. Each method has its own inherent advantages and drawbacks, which therefore dictates the most suitable measurement range for each technique [15]. In general, the direct method is not suitable for the measurement of low emissivity materials, due to the challenge of distinguishing the measurand's weak radiant power from internal instrument interferences, such as electronic noise. The indirect method is specifically to extend the measurement capabilities down to the lower emissivity region. However, this approach requires pre-investigation of the measurand's surface radiative properties, which poses different measurement challenges [16]. Until now, the boundary of the most suitable emissivity measurement range between the direct and indirect methods has not been systematically studied. Lack of a clear understanding of which method is more suitable for a particular measurement causes difficulties within the field of emissivity and non-contact temperature measurements using a radiation thermometer.

When undertaking emissivity measurements, researchers need to consider the uncertainties of the various measurement methods before selecting the most appropriate method for a particular measurement. When applying an emissivity value to a temperature measurement, users must have an appreciation of the uncertainty within the emissivity value in order to understand the reliability in the final measured temperature. Although the need for quantitative uncertainty comparison is necessary, few studies have reported due to two reasons. Firstly, the uncertainty estimation of published instruments is inadequate, resulting in an inability to compare results across publications [17-19]. Secondly, the uncertainty components in emissivity measurements derive from various sources using different measurement methods [20]. Insufficient quantitative uncertainty assessment of emissivity can lead to unknown temperature measurement errors, thereby impacting upon the accuracy of further measurements.

In this work, we present a new instrument for the measurement of emissivity which consists of a pair of hemispherical cups coated with Vantablack® and gold, respectively. Measurements were performed at temperatures ranging from 200 to 450 °C, operating over a spectral range of 2.1 to 2.5 μm. The instrument can offer three different measurement methods: direct, indirect, and in situ direct methods. The uncertainties within each method were assessed in order to evaluate which method is more suitable for different emissivity ranges. By selecting the most appropriate method, the expanded uncertainty of the instrument was lower than 0.058 at 200 °C and 0.030 at 450 °C (k = 2). Notably, using the indirect method at 450 °C, the expanded uncertainty was reduced as low as 0.014 for materials with emissivity of less than 0.18. Three commonly used materials [stainless steel 304 (SS304), aluminum alloy 6082 (Al6082), and the high emissivity paint HiE-Coat 840M] were measured to evaluate the performance of the instrument. The results indicated good agreement between design specifications and experimental results. Our instrument offers accurate emissivity measurements for use within radiation thermometry applications.

2. Experimental Setup

2.1 System description

Our instrument was designed to incorporate the measurement of emissivity by both direct and indirect methods. The instrument was composed of a Vantablack® coated cup (black-cup), gold coated cup (gold-cup), custom designed radiation thermometer, hot plate, and data acquisition system. The schematic diagram of the instrument is shown in Figure 1.

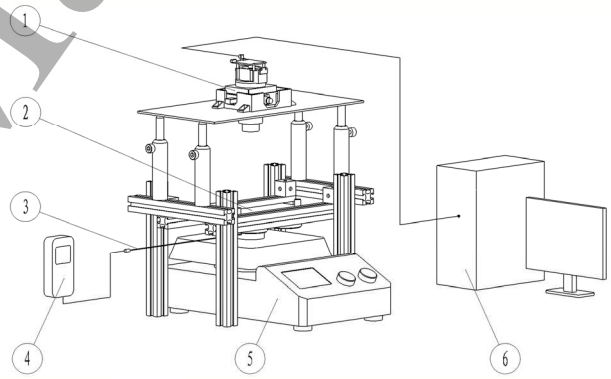

Figure 1. Schematic diagram of construction of the emissivity measurement instrument. Custom designed radiation thermometer (1); gold-black-cup unit (2); thermocouple, TC Direct 408-053 Class-1 (3); thermometer readout module, Fluke T3000 FC (4); hot plate, SCILOGEX MS7-H550-Pro (5); data acquisition system (6).

For each measurement, a sample was loaded on the central area of a hot plate positioned upon an optical bench. A thermocouple was inserted into a hole drilled into the sample to measure its temperature. This hole was 1.5 mm in diameter and 2 mm beneath the top surface. The black and gold cups were mounted upon a movable plate above the sample, assembling as a gold-black-cup unit. A 2 mm diameter hole was drilled at the top of each cup to allow the radiation emitted from the sample to pass through. The radiation thermometer, which was fixed at the top of the instrument, was focused onto

the position of the hole in order to receive the emitted radiation. The output signal of the thermometer was recorded by the data acquisition system.

The gold-black-cup unit was placed between a sample and the radiation thermometer, as shown in Figure 2. The cups were fabricated to be identical in shape, as shown in Figure 3. The internal surface of each cup was a half-sphere in shape, with a curvature of 20 mm in semi-diameter. The internal surface of the gold-cup was mirror polished and coated with gold to reflect the radiation emitted from a sample, leading to the emissivity enhancement. The internal surface of the black-cup was sand-blasted and coated Vantablack®-S-VIS (Surrey NanoSystems Ltd.) to block the background radiation from the hot plate, thereby acting as a radiation shield. The gold-black-cup unit can be slid along the optical rail between position A and B, allowing either the gold-cup or the black-cup to be positioned above a sample for its respective measurement.

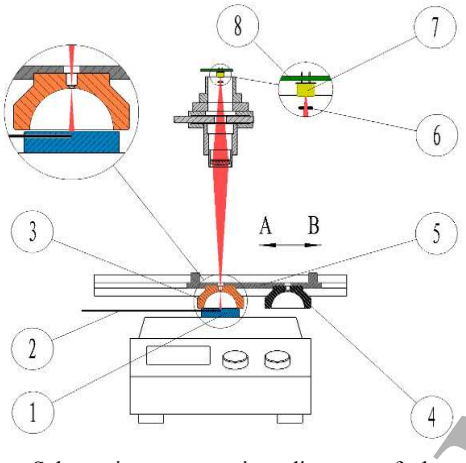

Figure 2. Schematic cross-section diagram of the emissivity measurement instrument. Sample (1); thermocouple (2); gold-cup (3); black-cup (4); movable plate (5); bandpass filter, 2.1 to 2.5 µm (6); Extended InGaAs photodiode, Hamamatsu G12183-010K (7); PCB (8).

The radiation thermometer consisted of a 60 mm focal length singlet lens, a bandpass filter, an extended indium gallium arsenide (Ex-InGaAs) photodiode, and a custom designed amplifier circuit upon a printed circuit board (PCB). The thermometer was designed as a common-path optical system with a red laser (650 nm) and the photodiode. The laser beam was used to align the focus position before each measurement. After alignment, the laser was powered off and the thermometer was changed to its radiation measurement mode. The parameters of the radiometer are listed in Table 1. The radiation thermometer was pre-calibrated with a blackbody furnace (LANDCAL P550P) from 200 to 450 °C at a working distance of 150 mm. The calibration data was stored as reference values for later emissivity measurements. The spectral responsivity of the radiation thermometer is shown in Figure 4.

Figure 3. Photo of the gold-cup and the black-cup mounted on a movable plate.

Table 1. Parameters of the radiation thermometer

Wavelength	2.1 to 2.5 µm
Focal length	60 mm
F-number	3.0
Working distance	150 mm
Field of view (design)	80:1
Spot size at working distance (design)	1.875 mm in diameter

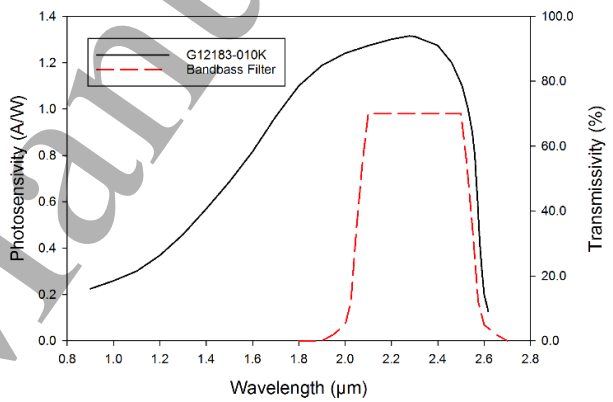

Figure 4. Spectral responsivity of the radiation thermometer. The left axis represents the photosensitivity of the Ex-InGaAs photodiode. The right axis represents the transmissivity of the bandpass filter.

2.2 Measurement procedures

Five sets of samples were prepared and measured, including rough SS303, rough Al6082, polished SS304, polished Al6082, and HiE-Coat 840M paint on an Al6082 substrate. The samples were machined to be 50 mm in diameter by 10 mm in thickness. A 1.5 mm diameter hole was drilled 2 mm from the top surface of the sample for insertion of the thermocouple. The depth of the hole was 25 mm, enabling the thermocouple tip to reach the sample's centre. Rough samples were ground by P240 sandpaper. Polished samples were ground by P240, P400, P800 sandpapers and polished to 3 µm by diamond suspensions. These samples were ultrasonically cleaned using isopropyl alcohol. The HiE-Coat 840M painted samples were ground by P240 sandpaper, cleaned by isopropyl alcohol and then brushed by the paint.

The thickness of the paint was approximately 0.15 to 0.20 mm. All samples were fully dried and stored in a vacuum box prior to measuring.

The prepared sample was positioned on the centre of the hot plate. The distance between the sample's top surface to the cup's bottom surface was adjusted to approximately 1 mm. Once the sample was loaded to the correct position, a thermocouple was inserted into the sample, enabling the commencement of the emissivity measurement.

The hot plate was set to the first temperature point. After the sample had stabilised at the measurement temperature for 30 min, the gold-cup was slid to cover the sample to gather the first set of data. The black-cup was then quickly moved to cover the sample to gather the second set of data. The sample's temperature was stored for both measurements. This process was repeated with the hot plate set at incremental temperature points until the whole series of measurements was collected. Figure 5 shows a picture of the instrument for measuring emissivity at 300 °C.

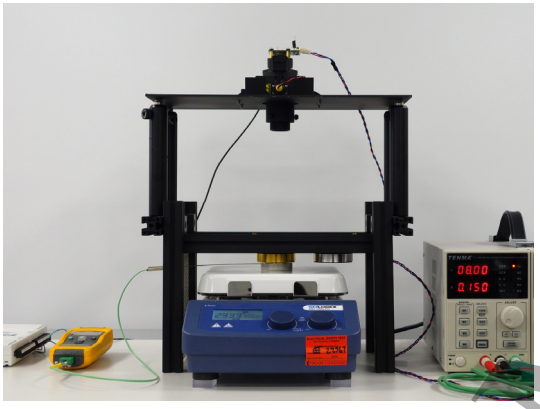

Figure 5. Picture of the instrument for the emissivity measurement of an aluminium sample at 300 °C.

3. Methodology

Our instrument was designed with the intention of measuring emissivity using three methods: the black-cup method, the gold-cup method, and the dual-cup method. The black-cup method is a direct emissivity measurement method. The normal emissivity is computed by measuring radiant power emitted from a sample when it is covered by the black-cup compared to that from a blackbody. The gold-cup method is an indirect measurement method. The enhanced effective emissivity of a sample is measured when it is covered by the gold-cup for computing the sample's original emissivity. The dual-cup method is characterised as an in situ direct measurement method. When this method is applied, the normal emissivity is computed using the ratio of radiant power from a sample when it is covered by the black-cup to that when covered by the gold-cup. This method does not require the pre-measured data of a blackbody furnace, unlike the other two methods.

3.1 Black-cup method

The black-cup method computes the ratio of radiant power emitted from a sample to that from a blackbody at the same temperature, wavelength, and viewing condition [6]. The radiant power from a blackbody furnace has been pre-measured from 200 to 450 °C, with temperature steps of 50 °C. When the sample is heated to the calibration temperature, the normal emissivity of a sample, $\varepsilon_s(\lambda, T)$, can be expressed as

$$\varepsilon_s(\lambda, T) = \frac{L_s(\lambda,T)}{L_b(\lambda,T)} \quad (1)$$

where λ is the wavelength, T is the temperature, $L_s(\lambda, T)$ is the the radiance from a sample, and $L_b(\lambda, T)$ is the radiance from a blackbody.

The spectral radiance of a blackbody, $L_b(\lambda, T)$, can be expressed by Planck's Law [6]

$$L_b(\lambda, T) = \frac{C_1}{\lambda^5(e^{C_2/\lambda T}-1)} \quad (2)$$

where $C_1 = 1.191 \times 10^8\ W \cdot \mu m^4 \cdot m^{-2} \cdot Sr^{-1}$ is the first radiation constant, and $C_2 = 1.439 \times 10^4\ \mu m \cdot K$ is the second radiation constant.

In practice, a radiation thermometer receives radiation not only from the sample, but also from its surroundings due to reflection and scattering. For example, radiation emitted from the hot plate may reflect onto the sample's surface, leading to the enhancement of measured emissivity. The measured emissivity, $\varepsilon_m(\lambda, T)$, can be described as

$$\varepsilon_m(\lambda, T) = \frac{L_s(\lambda,T)+L_{sur}(\lambda,T)}{L_b(\lambda,T)} \quad (3)$$

where $L_{sur}(\lambda, T)$ is the radiance from the surroundings.

To block the background radiation, a cold black-cup is used to cover the sample's surface during the measurement. If the measurement is taken quickly, the temperature change of a sample and the black-cup can be omitted. The measured emissivity thereby can represent the sample's emissivity.

$$\varepsilon_s(\lambda, T) \approx \varepsilon_m(\lambda, T) = \frac{L_{bc}(\lambda,T)}{L_b(\lambda,T)} \quad (4)$$

where $L_{bc}(\lambda, T)$ is the radiance from a sample covered by the black-cup.

3.2 Gold-cup method

The gold-cup has been widely used for fast temperature measurements since 1951 [21]. Herein, a gold-cup is applied to enhance the radiative property of a sample. This kind of enhancement is beneficial for the measurement of low emissivity materials, which will be discussed in detail further on.

The gold-cup method takes three steps to obtain the emissivity of a sample. The first step is to measure the enhanced radiant power from the sample when it is covered by the gold-cup. The second step is to compute the enhanced effective emissivity by taking the ratio of the measured radiant power from the sample to that from a blackbody at the same temperature. Once the relationship between the sample's

emissivity and its enhanced emissivity is known, the true emissivity of the sample can be computed as the last step.

When a sample is covered by the gold-cup, the sample and the cup form an approximate cavity. Part of the radiation emitted from the sample is reflected or absorbed by the internal surface whilst the rest escapes from the cup hole or the gap between the cup and the sample. The reflected radiation then returns back to the sample's surface, forming multiple internal reflections within the cavity, until all radiation has either escaped or been absorbed. Both the emitted and the reflected radiation from the measurement area are gathered by the radiation thermometer, resulting in the emissivity enhanced measurement [16].

The relationship between the sample emissivity and the enhanced effective emissivity is dependent upon the reflection properties of sample surface. If the sample surface acts as a Lambertian surface, the surface reflection can be treated as directional-hemispherical reflection. If the sample surface acts as a specular surface, the reflection is treated as specular reflection. To simplify the discussion, these calculations assume that the sample surface either acts as a Lambertian surface or a specular surface. In practice, this assumption can be used to represent the majority of materials [6].

3.2.1 Lambertian surface

For a sample with a Lambertian surface, the radiation emitted or reflected from that surface remains constant at any viewing angle [6]. Therefore, the sample's surface emits and reflects radiation uniformly to the cup, including the gap and the cup hole. The gold-cup internal surface is assumed performing as specular reflection. The enhanced effective emissivity measured by the radiation thermometer can be expressed as

$$\varepsilon_{eff}(\lambda,T)=\frac{\varepsilon_s(\lambda,T)}{1-\rho_{cup}(\lambda,T)\rho_s(\lambda,T)[(A_{cup}-A_{ho})/(A_{cup}+A_{gap})]} \quad (5)$$

where A_{ho} is the area of the gold-cup hole opening, A_{gap} is the area of the gap between a sample and gold-cup, A_{cup} is the area of the gold-cup internal surface, $\varepsilon_s(\lambda,T)$ is the emissivity of the sample, $\rho_{cup}(\lambda,T)$ is the reflectivity of the gold-cup internal surface, and $\rho_s(\lambda,T)$ is the reflectivity of the sample.

To simplify the equation, we define the geometrical factor, A, as

$$A=(A_{cup}-A_{ho})/(A_{cup}+A_{gap}) \quad (6)$$

If an opaque sample can maintain itself in a local thermal equilibrium, the relationship between spectral hemispherical emissivity and spectral directional-hemispherical reflectivity can be assumed to obey Kirchhoff's law approximately [6, 22].

$$\varepsilon_\theta(\lambda,T)=1-\rho_\theta(\lambda,T) \quad (7)$$

where $\varepsilon_\theta(\lambda,T)$ is the spectral directional emissivity which is equal to the spectral hemispherical emissivity for a Lambertian surface, and $\rho_\theta(\lambda,T)$ is the spectral directional-hemispherical reflectivity.

Once the enhanced effective emissivity is measured, the sample's emissivity can be computed by equations (5) and (7), expressed as

$$\varepsilon_s(\lambda,T)=\frac{\varepsilon_{eff}(\lambda,T)(1-\rho_{cup}(\lambda,T)A)}{1-\varepsilon_{eff}(\lambda,T)\rho_{cup}(\lambda,T)A} \quad (8)$$

In equation (6), the geometrical factor can be obtained from the shape of the gold-cup. The reflectivity of a polished gold surface is 0.96 over the spectral range of 2.1 to 2.5 μm [23]. Therefore, the relationship between the enhanced effective emissivity and the sample's emissivity is represented by the black line in Figure 7. When the emissivity of the sample increases from 0 to approximately 0.3, the enhanced effective emissivity increases from 0 to approximately 0.8, respectively. In turn, the enhanced effective emissivity increases from 0.8 to 1 when the sample emissivity increases from approximately 0.3 to 1. The gold-cup method offers a better minimum resolvable emissivity difference for low emissivity materials due to the radiation enhancement, and, therefore, improves the signal to noise ratio.

3.2.2 Specular surface

For a sample with a specular surface, its top surface obeys the law of reflection, similar to the internal surface of the gold-cup. The multi-reflection within the cavity, formed by the sample and the gold-cup, is dependent upon the incident angle of radiation. Therefore, the relationship described by equation (8) is not valid for very low emissivity materials and non-ideal experimental geometries.

A Monte Carlo ray-tracing method can be applied to determine the relationship in this case. The simulation is assumed to be a 2D model due to the symmetrical property of the cup. Firstly, the Ex-InGaAs photodiode sensor is replaced by an ideal blackbody surface, which randomly emits monochromatic rays into the gold-cup via the cup hole. The rays entering the cavity all fall within the radiation thermometer's field of view. The reflection of these rays within the cavity is then traced until all of them have either been absorbed or escaped from the cavity via the gap or the hole. Finally, by tracing large numbers of rays, the spectral absorptivity of a sample can be obtained as

$$\alpha_{eff}(\lambda,T)=N_{abs}/N \quad (9)$$

where N_{abs} is the number of rays absorbed by the sample's surface, and N is the number of rays entering the cavity.

According to Kirchhoff's law, once the spectral absorptivity of an object is known, the spectral emissivity under thermal equilibrium can be calculated:

$$\varepsilon_{eff}(\lambda,T)=\alpha_{eff}(\lambda,T) \quad (10)$$

where $\varepsilon_{eff}(\lambda,T)$ is the enhanced effective emissivity.

Figure 6(a) shows a ray that entered the cavity and escaped from the gap after multi-reflections. Figure 6(b) shows the tracing of 10,000 rays. The red dots in Figure 7 show the relationship between the sample's emissivity and enhanced effective emissivity. The data can be fitted by a seventh-order

polynomial equation, as shown in equation (11). The parameters and the residual fitting error, represented by root mean square error (RMSE), are shown in Table 2.

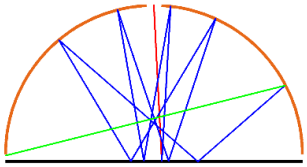

Figure 6(a). The pattern produced by tracing a single ray within the cup. The orange line is the internal surface of the gold-cup. The black line is the top surface of the sample. The red line represents the optical path of a ray entering the cup. The blue lines represent the optical paths of the ray reflecting within the cup. The green line represents the optical path of the ray escaping from the gap.

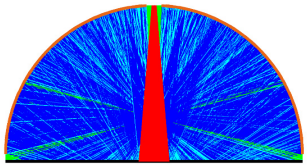

Figure 6(b). The pattern produced by tracing 10,000 rays within the cavity. The red area represents the field of view of the radiation thermometer. The blue area represents the internal reflections. The sky blue area represents the optical paths where rays are finally absorbed.

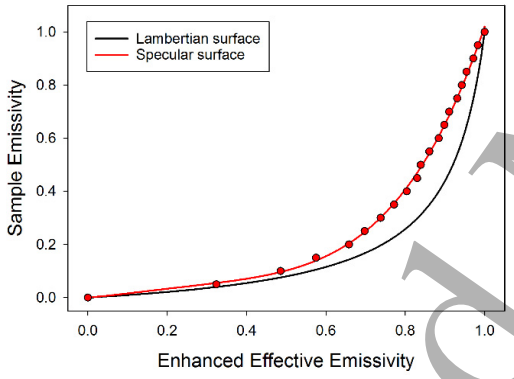

Figure 7. Relationship between the sample's emissivity and the enhanced effective emissivity. The black line represents the relationship of a Lambertian surface. The red line represents the relationship of a specular surface.

$$\varepsilon_s = P1 \times \varepsilon_{eff}^7 + P2 \times \varepsilon_{eff}^6 + P3 \times \varepsilon_{eff}^5 + P4 \times \varepsilon_{eff}^4 + P5 \times \varepsilon_{eff}^3 + P6 \times \varepsilon_{eff}^2 + P7 \times \varepsilon_{eff} + P8 \quad (11)$$

Table 2. Parameters of fitting curve for gold-cup method (specular surface)

Parameter	Value
P1	−0.7890
P2	1.5989
P3	−0.0423
P4	0.0478
P5	0.0127
P6	0.0696
P7	0.1209
P8	0.0000
RMSE	0.01121

3.3 Dual-cup method

In the previous two methods, the surface temperature of the sample is measured by the embedded thermocouple within the sample. A thermal gradient along the sample's vertical direction is inevitable due to the nature of the heating process, which causes the true surface temperature to be lower than the value measured by the thermocouple. This poses a challenge in selecting the reference temperature of the blackbody furnace for the computation of emissivity, thereby increasing the measurement uncertainty.

The dual-cup method can be applied to address this problem. Once the relationship between the sample's emissivity and enhanced effective emissivity is understood, the assembled cavity can be corrected to be an approximate blackbody. In that case, a sample is both the measurand and reference blackbody source. Equation (4) is now expressed as

$$\varepsilon_s(\lambda,T) = \frac{L_{bc}(\lambda,T)}{L_{gc}(\lambda,T)} \times \frac{L_{gc}(\lambda,T)}{L_b(\lambda,T)} \quad (12)$$

where $L_{bc}(\lambda,T)$ is the radiance from the sample covered by the black-cup, $L_{gc}(\lambda,T)$ is the radiance from the sample covered by the gold-cup, and $L_b(\lambda,T)$ is the radiance from a blackbody furnace.

Equation (12) can be rewritten in emissivity form as

$$\varepsilon_s(\lambda,T) = \varepsilon_{dual}(\lambda,T) \times \varepsilon_{eff}(\lambda,T) \quad (13)$$

where $\varepsilon_{dual}(\lambda,T)$ is the measured emissivity, which is the ratio of radiant power from a sample covered by the black-cup to that covered by the gold-cup, and $\varepsilon_{eff}(\lambda,T)$ is the enhanced effective emissivity of the cavity formed by a sample and the gold-cup.

By applying the dual-cup method, the enhanced effective emissivity performs as a correction factor which is independent of the measurement temperature. The enhanced effective emissivity can be obtained by equations (5) or (11), depending upon the sample surface reflection.

If a sample acts as a Lambertian surface, the emissivity can be calculated from equations (5) and (13), as

$$\varepsilon_s(\lambda,T) = \frac{\varepsilon_{dual}(\lambda,T) + A\rho_{cup}(\lambda,T) - 1}{A\rho_{cup}(\lambda,T)} \quad (14)$$

If a sample acts as a specular surface, the emissivity can be obtained by solution of equations (11) and (13). For the convenience of calculation, the result can be fitted by a fourth-order polynomial, as shown in equation (15). The parameters and the residual fitting error, represented by RMSE, are shown in Table 3.

$$\varepsilon_s = P1 \times \varepsilon_{dual}^4 + P2 \times \varepsilon_{dual}^3 + P3 \times \varepsilon_{dual}^2 + P4 \times \varepsilon_{dual} + P5 \quad (15)$$

Table 3. Parameters of fitting curve for dual-cup method (specular surface)

Parameter	Value
P1	1.4064
P2	−3.2416
P3	2.8000
P4	0.0374
P5	0.0000
RMSE	0.00479

4. Results and Discussion

4.1 Instrumental Uncertainty

This instrument was developed to carry out accurate emissivity measurements, which required an analysis of the instrumental uncertainties. The uncertainties of the instrument derive from four main sources: the radiance temperature error, background radiation interference, electronic noise, and systematic errors [24]. Systemic errors are due to the size of source effect (SSE) of the radiation thermometer, geometrical imperfection of cups, position change of samples for each measurement, and curve fitting error. Each emissivity measurement method utilised by the instrument has its own associated uncertainty components, which should be analysed separately. By studying the combined standard uncertainty and relative uncertainty, the most suitable emissivity measurement range of each method can be specified quantitatively.

In this work, the square of combined uncertainty $u_c(x)$ is expressed by equation (16) [20]. The uncertainty distribution is assumed to be a uniform distribution for all standard uncertainty components. The expanded uncertainty is expressed at approximately the 95% confidence level using a coverage factor of k = 2 [25]:

$$[u_c(x)]^2 = \sum_{i=1}^{N}[u(x_i)]^2 \quad (16)$$

where $u(x_i)$ is a standard uncertainty component.

4.1.1 Blackbody radiance temperature

The radiation thermometer was pre-calibrated by the blackbody furnace to provide reference values for both the black-cup and gold-cup methods. The radiance temperature uncertainty of the blackbody furnace for 200 to 450 °C was lower than ± 0.2 K. The uncertainty (k = 2) due to the blackbody radiance temperature error ranged from 0.00634 to 0.00274 over the measurement temperature range, as shown in Table 6.

4.1.2 Sample radiance temperature

The sample's temperature was monitored by a type K class 1 thermocouple embedded within the sample. As mentioned previously in section 3.3, the sample exhibited a vertical thermal gradient distribution due to the heating process, which resulted in the uncertainty in measuring the surface temperature of the sample. There were two components to this uncertainty: the thermocouple uncertainty and the vertical temperature difference between the thermocouple position and the sample top surface.

The thermocouple used in the instrument can measure temperature within an error range of ±1.5 °C over the temperature range of 0 to 375 °C and ±0.4% °C over the temperature range of 375 to 1000 °C. The uncertainty (k = 2) due to the thermocouple was from 0.04755 to 0.02470 between 200 °C and 450 °C.

The thermal properties of the samples, such as heat capacity, thermal conductivity and surface condition, contribute to the vertical temperature difference. This difference was analysed using Ansys Icepak for common materials. The maximum temperature difference (2.10 °C) occurred in SS304 at 450 °C, as shown in Table 4. Therefore, the maximum radiance temperature difference was estimated to be 2.5 °C. The uncertainty (k = 2) due to the temperature difference between the sample surface and the thermocouple readout ranged from 0.02265 to 0.02937, as shown in Table 6.

Table 4. Simulated temperature difference between the position of the thermocouple and centre of the sample surface

Material	Temperature variation (°C)			
	200 °C	300 °C	400 °C	450 °C
Al6802	−0.12	−0.21	−0.30	−0.35
SS304	−0.75	−1.29	−1.83	−2.10
Inconel	−0.69	−0.76	−0.83	−0.86
Copper	−0.05	−0.08	−0.12	−0.14
HiE-Coat 840M (painted on Al6082)	−0.66	−1.14	−1.62	−1.86
Estimated temperature difference	−0.83	−1.50	−2.17	−2.50

Note: The temperatures of 200, 300, 400, and 450 °C are the reference temperatures of the position of the thermocouple. The temperature variation indicates that the surface temperature of a sample is lower than the reference temperature.

4.1.3 Background radiation interference

For each measurement, a sample was heated to the measurement temperature and stabilised for 30 min before data acquisition started. During this period, the black-cup and the gold-cup were also exposed to the heating area of the hot plate, emitting background radiation to the sample after covering it. The radiation was reflected by the sample's surface, leading to the enhancement of the measured radiant power. The temperature increase of the black-cup and the gold-cup was simulated by Ansys Icepak across the entire measurement temperature range. The result is shown in Table 5, and the uncertainty (k = 2) due to the background radiation interference is shown in Table 6.

Table 5. Simulated temperature of gold-cup and black-cup

Cup	Simulated temperature (°C)			
	200 °C	300 °C	400 °C	450 °C
Gold-cup	50.14	70.80	94.33	107.07
Black-cup	41.30	55.52	71.27	79.78

4.1.4 Electronic noise

The radiation thermometer output fluctuated over the course of the measurement due to the electronic noise of photodiode-amplifier circuit, adding additional uncertainty to the measurement. This uncertainty increased at the lower end of the temperature range, due to the reduced signal-to-noise ratio of the measurement. The uncertainty (k = 2) due to thermometer noise ranged from 0.02834 to 0.00051 between

200 °C and 450 °C, as shown in Table 6.

4.1.5 Size of source effect

Size of source effect describes the phenomenon that a radiation thermometer measures radiation from the region outside of its nominal measurement area due to optical aberrations, diffraction, reflection, and scattering [26]. The radiation thermometer, therefore, receives unwanted radiant power emitted from its surroundings, leading to additional uncertainty. In this work, SSE was measured using the direct method [27], which can be expressed as

$$\sigma_S(r, r_{max}) = \frac{S(r,L)}{S(r_{max},L)} \quad (17)$$

where r is the radius of the aperture, r_{max} is the size of the maximum aperture, L is the working distance, $S(r, L)$ is the signal at the radius r, and $S(r_{max}, L)$ is the signal at the maximum aperture.

The SSE for the radiation thermometer, measured at a furnace temperature of 450 °C, is shown in Figure 8. The actual measurement area was smaller than 2 mm in diameter which agreed with the design specification. The maximum uncertainty caused by SSE was estimated to be 0.0059 (k = 2).

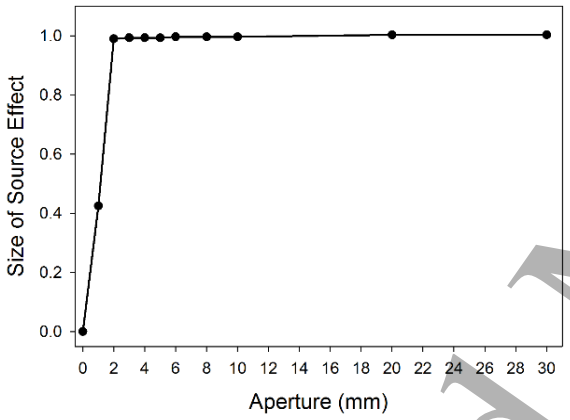

Figure 8. SSE of the radiometer measured at 450 °C with a working distance of 150 mm. SSE was close to 1 when the aperture was greater than 2 mm in diameter.

4.1.6 Geometrical imperfection

Geometrical imperfections within the shape of the cups can have a direct impact upon the measurement of the emissivity, particularly when using the gold cup. This imperfection was due to tolerances within the manufacturing process of the cups. For our instrument, the internal surface of the cups was required to be polished to 20 ± 0.02 mm in semi-diameter, whilst the hole at the top of the cups was required to be machined to between 2.00 and 2.05 mm in diameter. The maximum uncertainty (k = 2) due to the geometrical imperfection was estimated to be 0.00115.

4.1.7 Positioning

Working distance variations between the design specification and the actual working distance, leading to a measurement area change, contributed an additional measurement uncertainty. The positional uncertainty of the working distance variation was estimated to be ± 1 mm, with a maximum uncertainty (k = 2) estimated to be 0.0154.

4.1.8 Curve fitting error

The use of polynomial equations to fit the relationship between the enhanced effective emissivity and the sample's emissivity introduced a residual curve fitting error uncertainty. As analysed in Table 2 and Table 3, the maximum uncertainty was 0.01121 for the gold-cup method and 0.00479 for the dual-cup method (k = 2).

4.1.9 Expanded uncertainty

For all the uncertainty components discussed above, the overall uncertainty of the measurements can be calculated using equation (16). The expanded uncertainty (k = 2) was lower than 0.00580 at 200 °C, reducing to lower than 0.00301 at 450 °C, as shown in Table 6. The result for the gold-cup method only represents the uncertainty analysis for enhanced effective emissivity, which should be converted to relative expanded uncertainty for a direct comparison with the other two methods.

4.1.10 Relative expanded uncertainty

The relative expanded uncertainty (k = 2) at 200 °C and 450 °C are shown in Figures 9 and 10, respectively. Compared to the black-cup method, the dual-cup method consistently demonstrated the lower uncertainty. For materials with a Lambertian surface, which can represent the common surface property in various typical samples, each method had a distinct suitable emissivity measurement range. The gold-cup method was more suitable for the emissivity range of up to 0.22 at 200 °C, and up to 0.18 at 450 °C. The other two methods were found to be less uncertain under the other emissivity range. The lowest relative expanded uncertainty achieved by the gold-cup method was 23.08% at 200 °C and 15.39% at 450 °C, which was equivalent to the expanded uncertainty of 0.02136 and 0.01424 (k = 2). The lowest relative expanded uncertainty achieved by the dual-cup method was 5.80% at 200 °C and 3.01% at 450 °C (k = 2). With careful selection of the most appropriate emissivity measurement method, our instrument can achieve low measurement uncertainties over the emissivity range of 0.06 to 1.

Table 6. Expanded uncertainty (k = 2)

Uncertainty	Black-cup method Temperature (°C)				Dual-cup method Temperature (°C)			
	200	300	400	450	200	300	400	450
Blackbody radiance temperature	0.00634	0.00434	0.00316	0.00274	N/A	N/A	N/A	N/A
Sample thermocouple	0.04755	0.03258	0.02529	0.02470	0.04755	0.03258	0.02529	0.02470
Temperature difference on a sample	0.02265	0.02789	0.02932	0.02937	N/A	N/A	N/A	N/A
Background radiation (Gold-cup)	N/A	N/A	N/A	N/A	0.00010	0.00003	0.00002	0.00002
Background radiation (Black-cup)	0.00149	0.00035	0.00017	0.00013	0.00149	0.00035	0.00017	0.00013
Electronic Noise	0.02834	0.00313	0.00073	0.00051	0.02834	0.00313	0.00073	0.00051
SSE	0.00590	0.00590	0.00590	0.00590	0.00590	0.00590	0.00590	0.00590
Geometrical imperfection	0.00115	0.00115	0.00115	0.00115	0.00115	0.00115	0.00115	0.00115
Positioning	0.01540	0.01540	0.01540	0.01540	0.01540	0.01540	0.01540	0.01540
Curve fitting I	N/A	N/A	N/A	N/A	N/A	N/A	N/A	N/A
Curve fitting II	N/A	N/A	N/A	N/A	0.00479	0.00479	0.00479	0.00479
Expanded uncertainty	**0.06240**	**0.04627**	**0.04223**	**0.04188**	**0.05799**	**0.03698**	**0.03060**	**0.03011**

Uncertainty	Gold-cup method Specular surface, Temperature (°C)				Gold-cup method Lambertian surface, Temperature (°C)			
	200	300	400	450	200	300	400	450
Blackbody radiance temperature	0.00634	0.00434	0.00316	0.00274	0.00634	0.00434	0.00316	0.00274
Sample thermocouple	0.04755	0.03258	0.02529	0.02470	0.04755	0.03258	0.02529	0.02470
Temperature difference on a sample	0.02265	0.02789	0.02932	0.02937	0.02265	0.02789	0.02932	0.02937
Background radiation (Gold-cup)	0.00010	0.00003	0.00002	0.00002	0.00010	0.00003	0.00002	0.00002
Background radiation (Black-cup)	N/A	N/A	N/A	N/A	N/A	N/A	N/A	N/A
Electronic Noise	0.02834	0.00313	0.00073	0.00051	0.02834	0.00313	0.00073	0.00051
SSE	0.00590	0.00590	0.00590	0.00590	0.00590	0.00590	0.00590	0.00590
Geometrical imperfection	0.00115	0.00115	0.00115	0.00115	0.00115	0.00115	0.00115	0.00115
Positioning	0.01540	0.01540	0.01540	0.01540	0.01540	0.01540	0.01540	0.01540
Curve fitting I	0.01121	0.01121	0.01121	0.01121	N/A	N/A	N/A	N/A
Curve fitting II	N/A	N/A	N/A	N/A	N/A	N/A	N/A	N/A
Expanded uncertainty	**0.06338**	**0.04761**	**0.04369**	**0.04335**	**0.06238**	**0.04627**	**0.04223**	**0.04188**

Note: The expanded uncertainty of gold-cup method is evaluated for enhanced effective emissivity.

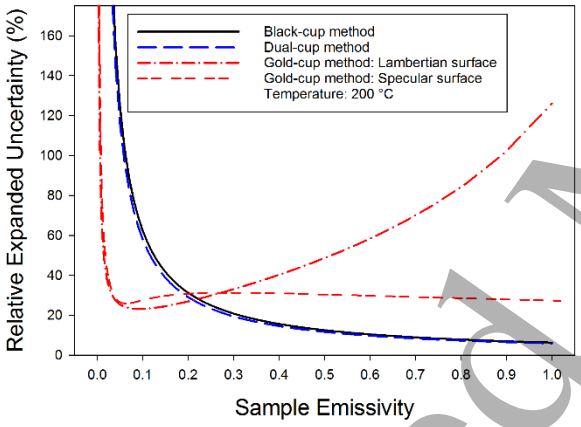

Figure 9. Relative expanded uncertainty at 200 °C (k = 2).

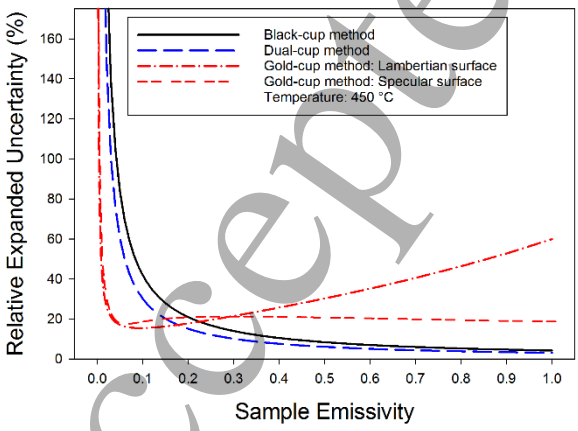

Figure 10. Relative expanded uncertainty at 450 °C (k = 2).

4.2 Results of emissivity measurements on SS304, Al6082, and HiE-Coat 840M

To evaluate the performance of our instrument, five sets of samples were measured, including rough SS303, rough Al6082, polished SS304, polished Al6082, and HiE-Coat 840M paint on an Al6082 substrate. These samples can represent materials ranging from low emissivity values to high emissivity values over the spectral range of 2.1 to 2.5 µm, according to previously published studies [28-30]. Samples were heated to the measurement temperatures, ranging from 200 to 450 °C, in sequential steps of 50 °C. All samples were exposed to air during measurements, leading to the measured emissivity being accompanied by surface oxidisation. Figure 11 shows the samples before and after the measurement. The colour of the SS304 samples changed from light grey to light brown, whereas the colour of the other samples was remained the same.

Figure 12 shows the emissivity of polished Al6082 from 200 to 450 °C. The three measurement methods produced different results. The emissivity measured by the gold-cup method increased from 0.1080 at 200 °C to 0.1692 at 350 °C, before stabilising to approximately 0.16 from 350 °C to 450 °C. The emissivity measured by the black-cup method increased from 0.0903 at 200 °C to 0.1347 at 350 °C and then decreased to 0.1117 at 450 °C. The emissivity measured by the dual-cup method increased from 0.0779 to 0.1135 at 350 °C and then decreased to 0.0089 at 450 °C.

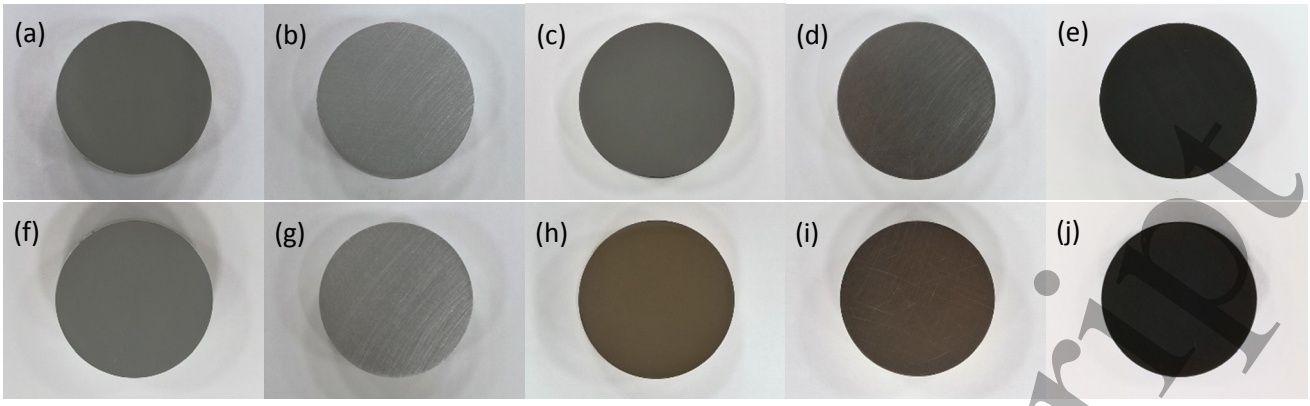

Figure 11. Pictures of samples before and after the emissivity measurement: (a) to (e) are samples before the measurement, and (f) to (j) are samples after the measurement; (a) and (f) are polished Al6082; (b) and (g) are rough Al6082; (c) and (h) are polished SS304; (d) and (i) are rough SS304; (e) and (j) are HiE-Coat 840M painted on Al6082.

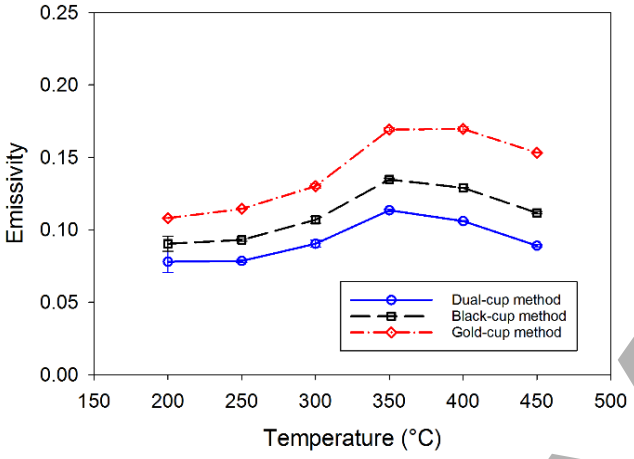

Figure 12. Emissivity of polished Al6082.

Figure 13 shows the emissivity of rough Al6082 between 200 °C and 450 °C. The gold-cup method showed an increase in emissivity from 0.1415 at 200 °C to 0.1824 at 450 °C. Both the black-cup and dual-cup methods indicated that emissivity values were constant at approximately 0.15 over the entire measurement temperature range.

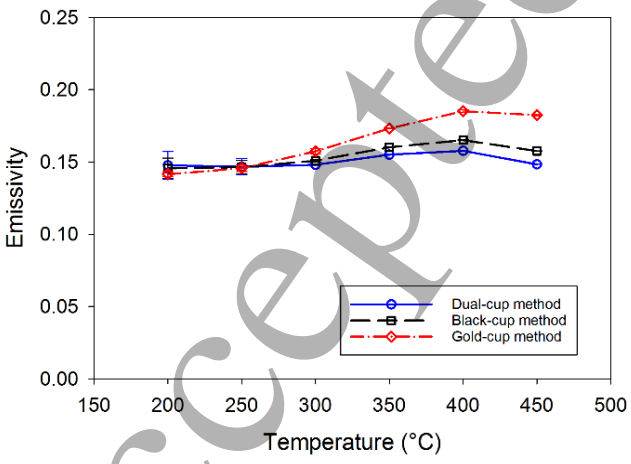

Figure 13. Emissivity of rough Al6082.

Figure 14 shows the emissivity of polished SS304 between 200 °C and 450 °C. Similar to the result of polished Al6082, the three methods showed different emissivity performances. The gold-cup method indicated that emissivity increased continuously from 0.2649 at 200 °C to 0.3162 at 450 °C. The black-cup method measured the emissivity to be stable at approximately 0.22 over the measurement temperature range, whilst the dual-cup method indicated that emissivity was stable at approximately 0.2.

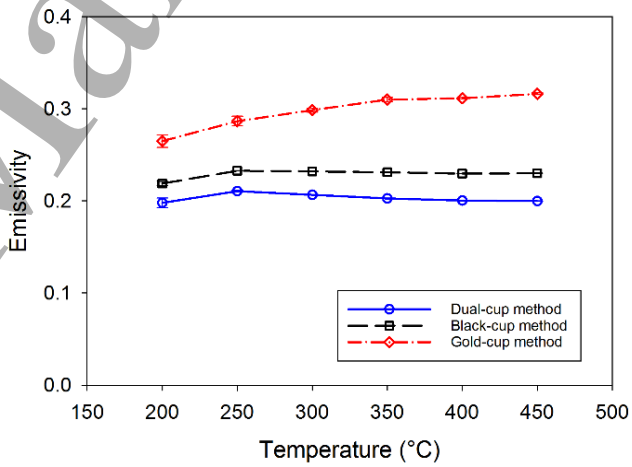

Figure 14. Emissivity of polished SS304.

Figure 15 shows the emissivity of rough SS304 from 200 to 450 °C. The three methods showed a similar trend of emissivity value over the measurement temperature range: emissivity was constant at approximately 0.3 from 200 to 300 °C and then increased to approximately 0.38 at 450 °C.

Figure 16 shows the emissivity of HiE-Coat 840M paint from 200 to 450 °C. The results of the gold-cup method were not valid due to the inherent methodology and, therefore, not included in the figure. Both the black-cup and dual-cup methods showed a similar trend in emissivity, with decreased emissivity from approximately 0.92 to 0.90 from 200 to 450 °C.

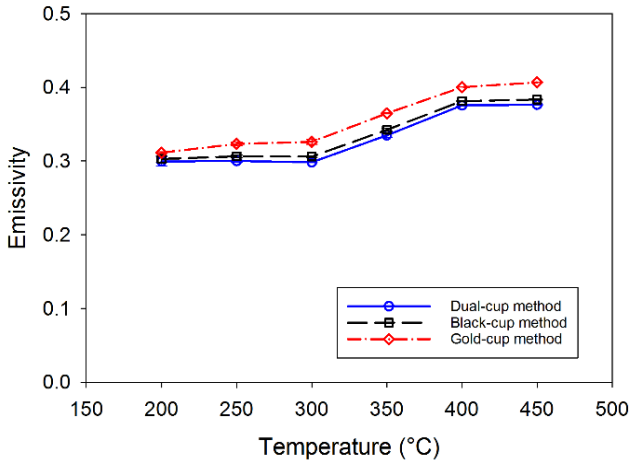

Figure 15. Emissivity of rough SS304.

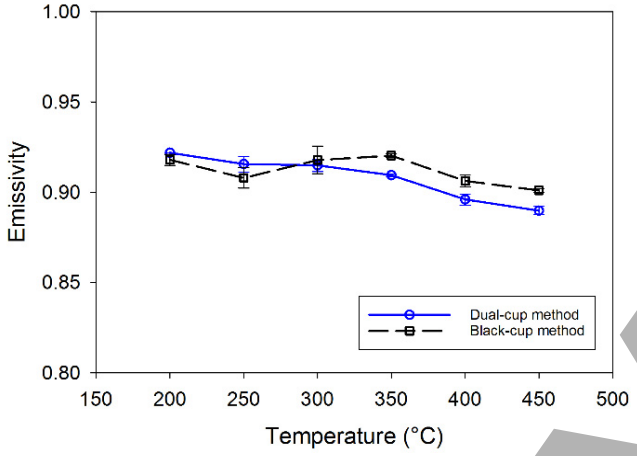

Figure 16. Emissivity of HiE-Coat 840M paint.

4.3 Discussion

The samples which have been measured (SS304, A16082, and HiE Coat 840M) cover a wide range of emissivities; observation of these materials enabled us to evaluate the performance of our instrument. The emissivity of polished Al6082 was within the range of 0.07 to 0.17 over the entire temperature range using all three methods. Similarly, the emissivity of rough Al6082 was consistently measured to be within the range of 0.14 to 0.20. The emissivity of polished SS304 ranged from 0.19 to 0.35 across the measurement methods, whilst the emissivity of rough SS304 ranged from 0.30 to 0.45. For HiE-Coat 840M painted Al6082, the emissivity ranged from 0.90 to 0.92 across the temperature range for both methods assessed. The results of our emissivity measurements were compared with published results. Although the comparison could not be undertaken under identical measurement conditions, such as the temperature, wavelength, measurement environment, and surface condition, this comparison can offer a straightforward evaluation of our instrument. Our emissivity measurements of these materials generally agree with published measurements of stainless steel [28], aluminium alloy [29], and HiE-Coat 840M paint within the literature [30]. This, therefore, validates our results and instrument's approach to emissivity measurements.

Each measurement method has its own most suitable emissivity measurement range, as discussed in section 4.1. Figures 12, 13, and 14 show that the radiative properties of low emissivity materials, such as the polished Al6082, polished SS304 and rough Al6082, were different between the gold-cup method and the other two methods. The gold-cup method indicated that the emissivity value of these samples increased with rise in temperature, whereas the other two methods indicated constant emissivity. After performing the measurement, samples were cooled to 200 °C and their emissivities were re-measured. It was found that the measured emissivities did not return to their original values, indicating that surface oxidisation of the samples played a dominant role in the emissivity increase. This is consistent with previous studies which also observed a relationship between the surface oxidisation and increase in emissivity for stainless steel and aluminium alloys after a long heating period [31, 32]. For our measurements, this kind of emissivity increase was only observed in the gold-cup method, which supported the argument that the gold-cup method can offer a better measurement approach than the other two methods for low emissivity materials.

For middle and high emissivity materials, such as the rough SS304 and HiE-Coat 840M paint, emissivity values measured by the black-cup and dual-cup methods agreed with each other, as shown in Figures 15 and 16. The increase in the emissivity of rough SS304 was observed using all three methods. Similarly, the measured emissivity values following the cooling phase did not return to the originally measured values at 200 °C. This again indicated that surface oxidisation impacted emissivity measurements. Our results demonstrated that both the black-cup and dual-cup methods can offer a lower uncertainty for measuring the measurement of middle and high emissivity materials.

The surface condition of the metal samples, Al6082 and SS304, measured in this work changed during the measurement in terms of chemical composition and surface roughness. Oxidisation of metal samples is a common phenomenon which depends on many factors such as the temperature, oxidisation period, humidity, and air flow speed. Thus, emissivity may have been affected by changes in the surface condition during the process of obtaining the results in this work.

5. Conclusion

We presented an instrument for emissivity measurements between temperatures of 200 to 450 °C over a spectral range of 2.1 to 2.5 µm using three different methods. The expanded

uncertainty of our instrument is lower than 0.058 at 200 °C and 0.030 at 450 °C (k = 2). By thoroughly analysing the various sources of uncertainty, the most suitable measurement range of each method has been quantitatively assessed and determined. The gold-cup method is better for the measurement of low emissivity materials, whereas the black-cup and dual-cup methods are suitable for all other emissivity ranges. With careful selection of the most appropriate measurement method for a specific application, our instrument can achieve very low relative expanded uncertainty. The capability of our instrument will enable accurate emissivity measurements for various materials used within radiation thermometry applications. Future developments will be to extend the range of measurement temperatures and wavelengths of the instrument, enabling further capabilities for more comprehensive emissivity studies.

Acknowledgments

Engineering and Physical Sciences Research Council (EPSRC) fellowship EP/M009106/1, Dr. Jon R. Willmott.

Reference

[1] Cai L, Song A Y, Wu P, Hsu P C, Peng Y, Chen J, Liu C, Catrysse P B, Liu Y, Yang A, Zhou C, Zhou C, Fan S and Cui Y 2017 Warming up human body by nanoporous metallized polyethylene textile *Nat Commun* **8** 496

[2] Boone N, Zhu C, Smith C, Todd I and Willmott J R 2018 Thermal near infrared monitoring system for electron beam melting with emissivity tracking *Addit. Manuf.* **22** 601-5

[3] Martinek J, Valtr M, Hortvík V, Grolich P, Briand D, Shaker M and Klapetek P 2019 Large area scanning thermal microscopy and infrared imaging system *Meas. Sci. Technol.* **30** 035010

[4] Araújo A 2017 Multi-spectral pyrometry—a review *Meas. Sci. Technol.* **28** 082002

[5] Madding R P 1999 Emissivity measurement and temperature correction accuracy considerations. In: *Thermosense XXI*: International Society for Optics and Photonics) pp 393-401

[6] Howell J R and Siegel R 1992 *Thermal radiation heat transfer* (New York: Hemisphere Publishing Co.)

[7] Monte C, Gutschwager B, Morozova S P and Hollandt J 2008 Radiation Thermometry and Emissivity Measurements Under Vacuum at the PTB *Int. J. Thermophys.* **30** 203-19

[8] Pérez-Sáez R B, Campo L d and Tello M J 2008 Analysis of the Accuracy of Methods for the Direct Measurement of Emissivity *Int. J. Thermophys.* **29** 1141-55

[9] Hanssen L M, Mekhontsev S N and Khromchenko V B 2004 Infrared spectral emissivity characterization facility at NIST. In: *Thermosense XXVI*: International Society for Optics and Photonics) pp 1-12

[10] Honnerová P, Martan J, Kučera M, Honner M and Hameury J 2014 New experimental device for high-temperature normal spectral emissivity measurements of coatings *Meas. Sci. Technol.* **25** 095501

[11] Riou O, Guiheneuf V, Delaleux F, Logerais P-O and Durastanti J-F 2016 Accurate methods for single-band apparent emissivity measurement of opaque materials *Measurement* **89** 239-51

[12] Králík T, Musilová V, Hanzelka P and Frolec J 2016 Method for measurement of emissivity and absorptivity of highly reflective surfaces from 20 K to room temperatures *Metrologia* **53** 743-53

[13] Vishnevetsky I, Rotenberg E, Kribus A and Yakir D 2019 Method for accurate measurement of infrared emissivity for opaque low-reflectance materials *Appl. Opt.* **58** 4599-609

[14] Honnerova P, Martan J, Vesely Z and Honner M 2017 Method for emissivity measurement of semitransparent coatings at ambient temperature *Sci. Rep.* **7** 1386

[15] Wang L P, Basu S and Zhang Z M 2011 Direct and Indirect Methods for Calculating Thermal Emission From Layered Structures With Nonuniform Temperatures *J. Heat Transfer* **133** 072701

[16] Zhang Z M, Tsai B K and Machin G 2009 *Radiometric Temperature Measurements: II. Applications* vol 43 (Cambridge, MA: Academic Press)

[17] Wen C-D and Mudawar I 2006 Mathematical determination of emissivity and surface temperature of aluminum alloys using multispectral radiation thermometry *Int. Commun. Heat Mass Transfer* **33** 1063-70

[18] Goett G, Kozakov R, Uhrlandt D, Schoepp H and Sperl A 2013 Emissivity and temperature determination on steel above the melting point *Weld. World* **57** 595-602

[19] Wang P, Hu Z, Xie Z and Yan M 2018 A new experimental apparatus for emissivity measurements of steel and the application of multi-wavelength thermometry to continuous casting billets *Rev. Sci. Instrum.* **89** 054903

[20] 1995 *Guide to the Expression of Uncertainty in Measurement (GUM)* (Geneva: International Organisation for Standardisation)

[21] Drury M D, Perry K P and Land T 1951 Pyrometers for surface-temperature measurement *J. Iron Steel Inst.* **169** 245-50

[22] Fu T, Duan M, Tang J and Shi C 2015 Measurements of the directional spectral emissivity based on a radiation heating source with alternating spectral distributions *Int. J. Heat Mass Transfer* **90** 1207-13

[23] Edmund Optics Ltd 2019 Metallic Mirror Coatings. Nether Poppleton, UK [Online]. Available: https://www.edmundoptics.eu/resources/application-notes/optics/metallic-mirror-coatings/

[24] Fischer J, Battuello M, Sadli M, Ballico M, Park S N, Saunders P, Zundong Y, Johnson B C, Ham E v d, Li W, Sakuma F, Machin G, Fox N, Ugur S and Matveyev

M 2003 Uncertainty budgets for realisation of scales by radiation thermometry [Online]. Available: https://www.bipm.org/cc/CCT/Allowed/22/CCT03-.pdf

[25] del Campo L, Pérez-Sáez R B, González-Fernández L and Tello M J 2010 Combined standard uncertainty in direct emissivity measurements *J. Appl. Phys.* **107** 113510

[26] Yoon H W, Allen D W and Saunders R D 2005 Methods to reduce the size-of-source effect in radiometers *Metrologia* **42** 89-96

[27] Saunders P and Edgar H 2009 On the characterization and correction of the size-of-source effect in radiation thermometers *Metrologia* **46** 62-74

[28] Shurtz R 2018 Total Hemispherical Emissivity of Metals Applicable to Radiant Heat Testing. (Albuquerque, NM, United States: Sandia National Lab. (SNL-NM))

[29] Lanc Z, Zeljković M, Štrbac B, Živković A, Drstvenšek I and Hadžistević M 2015 The Determination of the Emissivity of Aluminum Alloy AW 6082 Using Infrared Thermography *J. Prod. Eng.* **18** 23-6

[30] Aremco Products Inc. 2015 High Temperature Specialty Coatings. Valley Cottage, N.Y. www.aremco.com/wp-content/uploads/2015/06/TechNote-840-M.pdf

[31] Wen C-D and Mudawar I 2005 Emissivity characteristics of polished aluminum alloy surfaces and assessment of multispectral radiation thermometry (MRT) emissivity models *Int. J. Heat Mass Transfer* **48** 1316-29

[32] Shi D, Zou F, Wang S, Zhu Z and Sun J 2014 Effect of surface oxidization on the spectral emissivity of steel 304 at the elevated temperature in air *Infrared Phys. Technol.* **66** 6-12